

# High-Resolution Variable-Temperature $^{31}\text{P}$ NMR of Solid Calcium Phosphates

W. P. Rothwell,<sup>§</sup> J. S. Waugh,\*<sup>§</sup> and J. P. Yesinowski<sup>†</sup>

Contribution from the Department of Chemistry, Massachusetts Institute of Technology, Cambridge, Massachusetts 02139, and the Miami Valley Laboratories, The Procter & Gamble Company, P.O. Box 39175, Cincinnati, Ohio 45247. Received October 29, 1979

**Abstract:** We have used  $^{31}\text{P}$  NMR magic-angle sample spinning and proton enhancement to characterize the following compounds: hydroxyapatite,  $\text{Ca}_{10}(\text{OH})_2(\text{PO}_4)_6$ , and its nonstoichiometric forms;  $\text{Ca}_{10}\text{F}_2(\text{PO}_4)_6$ ;  $\text{Ca}_8\text{H}_2(\text{PO}_4)_6 \cdot 5\text{H}_2\text{O}$ ;  $\text{CaHPO}_4 \cdot 2\text{H}_2\text{O}$ ;  $\text{Ca}(\text{H}_2\text{PO}_4)_2 \cdot \text{H}_2\text{O}$ ;  $\text{Ca}(\text{H}_2\text{PO}_4)_2$ ; and, as an example of mineralized tissue, dental enamel. The  $^{31}\text{P}$  isotropic chemical shifts tend to move upfield upon protonation of the phosphate. The chemical-shift anisotropy is small for  $\text{PO}_4^{3-}$  groups, but significantly larger for  $\text{HPO}_4^{2-}$  and  $\text{H}_2\text{PO}_4^-$  groups, where axially asymmetric shift tensors of a width  $\sim 100$ – $130$  ppm are observed. For  $\text{Ca}_8\text{H}_2(\text{PO}_4)_6 \cdot 5\text{H}_2\text{O}$ , an increase in the apparent shift anisotropy of the  $\text{HPO}_4^{2-}$  groups at  $-165$  °C suggests that some atomic or molecular motion is being partially frozen out. At room temperature the spectra of synthetic samples of nonstoichiometric hydroxyapatite with Ca/P as low as 1.33 closely resemble those of stoichiometric hydroxyapatite (Ca/P = 1.67). The nonstoichiometry in these samples does not result from the presence of additional compounds with Ca/P ratios less than 1.67. Rather, a scheme involving  $\text{Ca}^{2+}$  vacancies in a hydroxyapatite lattice with a concomitant loss of  $\text{OH}^-$  ions and addition of protons seems most consistent with the NMR results. These additional protons do not appear to form rigid, discrete  $\text{HPO}_4^{2-}$  groups. Spectra obtained at  $-180$  °C provide some evidence for motions involving the protonated phosphate in a hydroxyapatite lattice.

## Introduction

The  $^{31}\text{P}$  NMR chemical shifts of solid calcium phosphates offer a means of detecting and distinguishing these compounds in mineralized tissue such as bone and teeth, and of studying structural problems in calcium phosphate chemistry. Although the  $^{31}\text{P}$  resonances of these solids are normally too broad and structureless for these purposes, magic-angle spinning (MAS) combined with high-power proton decoupling results in high-resolution  $^{31}\text{P}$  NMR spectra from which various compounds may be distinguished by either their isotropic chemical shift or their chemical-shift anisotropies. Indeed, Herzfeld et al.<sup>1</sup> have recently used  $^{31}\text{P}$  MAS-NMR to detect  $\text{CaHPO}_4 \cdot 2\text{H}_2\text{O}$  and hydroxyapatite in density-separated bone fractions. Furthermore, variable-temperature  $^{31}\text{P}$  MAS-NMR can be used to study motions occurring in the solid state. We wish to report  $^{31}\text{P}$  MAS-NMR results obtained for a variety of well-characterized synthetic calcium phosphates of biological significance, including highly nonstoichiometric calcium hydroxyapatites.

Calcium and phosphate ions form a number of crystalline or amorphous compounds generically called "calcium phosphates." These compounds form a series of increasing basicity (i.e., precipitating from increasingly basic solutions of calcium and phosphate ions), with a concomitant increase in the Ca/P molar ratio and decrease in their solubility in water. Table I lists the important members of the series and their abbreviations.

Calcium hydroxyapatite,  $\text{Ca}_{10}(\text{OH})_2(\text{PO}_4)_6$ , is the most basic commonly occurring calcium phosphate, with a theoretical molar Ca/P ratio of 1.67. A form of calcium hydroxyapatite (HAP) is the major mineral constituent of bone and teeth. The chemical properties of bone mineral have been recently reviewed.<sup>2</sup> Molar Ca/P ratios less than the ideal 1.67 for stoichiometric hydroxyapatite are often observed in mineralized tissue.<sup>3</sup> Highly nonstoichiometric compounds with Ca/P ratios less than 1.67 can also be synthesized; they exhibit X-ray powder diffraction patterns characteristic of calcium hydroxyapatite, and are sometimes referred to as "calcium-deficient apatites". Various proposals that have been advanced for the structures of these nonstoichiometric apatites<sup>2,3</sup> are

discussed below in view of our  $^{31}\text{P}$  NMR results. These results also form a basis for the analysis of calcium phosphates in mineralized tissue; an example involving dental enamel is given.

The principles of magic-angle spinning (MAS) NMR and proton-enhanced NMR have been discussed previously.<sup>4,5</sup> We merely note that the dipolar coupling between  $^1\text{H}$  and  $^{31}\text{P}$  is utilized in a cross-polarization process to obtain a proton-enhanced  $^{31}\text{P}$  NMR signal (proton decoupled). The cross-polarization rate is faster for larger dipolar couplings. Spinning the sample rapidly ( $\sim 2$  kHz) about an axis at the so-called magic angle of  $54.7^\circ$  with respect to the magnetic field removes the remaining  $^{31}\text{P}$ – $^{31}\text{P}$  dipolar interactions and the  $^{31}\text{P}$  chemical-shift anisotropy. The result is a high-resolution  $^{31}\text{P}$  NMR signal possessing a set of sidebands at multiples of the spinning frequency. The intensity of these sidebands is greater the larger the chemical-shift anisotropy (at a constant spinning frequency).

## Experimental Section

**Synthesis and Characterization of Compounds.** The nonstoichiometric HAP samples were synthesized by the method of Bett, Christner, and Hall.<sup>6</sup> A phosphoric acid solution, which was purified by passage through an Amberlite IR-20 column in the acid form and stored in a quartz vial, was added over a period of 1 h to a  $\text{Ca}(\text{OH})_2$  solution in the desired ratio, and the precipitate was then heated to dryness. The samples were not washed. The CaO used to prepare the  $\text{Ca}(\text{OH})_2$  solution was prepared by flushing a quartz tube containing reagent-grade  $\text{CaCO}_3$  at 900 °C overnight with nitrogen gas that had been passed through a  $\text{CO}_2$  trap; the distilled water used for the solution was boiled while bubbling nitrogen gas through it. These precautions were necessary to prevent carbonate impurities in the HAP (one carbonate-containing HAP sample was synthesized without these precautions).

A stoichiometric sample of carbonate-free HAP prepared as previously described<sup>7</sup> was generously provided and characterized by Mr. B. Fowler of NIDR-NIH. Chemical analysis showed it to be stoichiometric (Ca/P =  $1.66 \pm 0.01$ ,  $<0.05\%$   $\text{CO}_3^{2-}$ ), and X-ray powder diffraction revealed that about 70% of the sample was in the monoclinic form characteristic of highly stoichiometric HAP.

A sample of OCP was synthesized by adding together at identical rates equal volumes of 0.026 M  $\text{CaCl}_2$  and 0.020 M  $\text{Na}_2\text{HPO}_4$  adjusted to pH 7.5, and allowing the precipitate to stand for 2 days before washing with doubly distilled water and drying.

DCPD, DCPA, and MCPM were obtained commercially. MCPA

<sup>§</sup> Massachusetts Institute of Technology.

<sup>†</sup> Procter & Gamble.

Table I. <sup>31</sup>P Chemical Shifts of Solid Calcium Phosphates

abbreviation	formula	name	theoretical Ca/P (molar)	<sup>31</sup> P isotropic chemical shift <sup>a</sup>	principal values of <sup>31</sup> P chemical shift <sup>a,b</sup>		
					σ <sub>11</sub>	σ <sub>22</sub>	σ <sub>33</sub>
HAP(1.66) <sup>c</sup>	Ca <sub>10</sub> (OH) <sub>2</sub> (PO <sub>4</sub> ) <sub>6</sub>	calcium hydroxyapatite	1.67	2.8 ± 0.2	19 ± 3	4 ± 6	-15 ± 1
HAP(1.58) <sup>c</sup>	unknown	nonstoichiometric calcium hydroxyapatite	variable	2.8 ± 0.2	19 ± 4	4 ± 3	-14 ± 1
HAP(1.46) <sup>c</sup>	unknown	hydroxyapatite	variable	2.8 ± 0.2			
HAP(1.33) <sup>c</sup>	unknown		variable	2.8 ± 0.2			
HAP(1.14) <sup>c</sup>	unknown		variable	2.8 ± 0.2			
FAP	Ca <sub>10</sub> F <sub>2</sub> (PO <sub>4</sub> ) <sub>6</sub>	(synthetic) fluoroapatite	1.67	2.8 ± 0.2			
OCP	Ca <sub>8</sub> H <sub>2</sub> (PO <sub>4</sub> ) <sub>6</sub> ·5H <sub>2</sub> O	octacalcium phosphate	1.33	3.4 ± 0.3			
DCPD	CaHPO <sub>4</sub> ·2H <sub>2</sub> O	dicalcium phosphate dihydrate	1.0	1.7 ± 0.3 9 <sup>f</sup>	70 ± 6 77 <sup>f</sup>	-12 ± 6 1 <sup>f</sup>	-53 ± 3 -50 <sup>f</sup>
DCPA	CaHPO <sub>4</sub>	dicalcium phosphate, anhydrous	1.0	0.0 ± 0.4 <sup>e</sup> -1.5 ± 0.4			
MCPM	Ca(H <sub>2</sub> PO <sub>4</sub> ) <sub>2</sub> ·H <sub>2</sub> O	monocalcium phosphate monohydrate	0.5	-0.1 ± 0.3 -4.6 ± 0.3	49 ± 4 59 ± 6	-1 ± 4 -7 ± 6	-48 ± 2 -66 ± 3
MCPA	Ca(H <sub>2</sub> PO <sub>4</sub> ) <sub>2</sub>	monocalcium phosphate, anhydrous	0.5	0.5 ± 0.4 -0.5 ± 0.4 <sup>e</sup>			

<sup>a</sup> In parts per million; positive shifts are downfield from 85% H<sub>3</sub>PO<sub>4</sub> reference. No bulk susceptibility corrections were made. <sup>b</sup> Calculated using moments analysis of sideband intensities (ref 4). Ignoring the effects of homonuclear dipolar couplings upon the analysis was justified by results for HAP obtained at a higher field (τ 7.05). Peak heights and/or integrated intensities were used, since for HAP(1.58) the principal values calculated using both methods agreed within experimental error. <sup>c</sup> Numbers in parentheses refer to the experimentally determined Ca/P ratios. <sup>d</sup> Minor component. <sup>e</sup> Shoulder on larger peak. <sup>f</sup> Average value from single-crystal study (ref 14).

was prepared by heating MCPM (washed with anhydrous ethanol to remove phosphoric acid contaminant) to 110 °C for 2 days.

A synthetic FAP sample produced by low-temperature precipitation and characterized<sup>8</sup> was kindly provided by Dr. E. C. Moreno of Forsyth Dental Center. The mineral FAP sample was a pale yellowish-green specimen from Durango, Mexico, that was ground to 325 mesh.

The identity of all samples was confirmed by comparison of the X-ray powder diffraction pattern with NBS data cards. The powdered human enamel sample exhibited an apatitic diffraction pattern. IR and Raman spectra of the HAP samples, and IR spectra of OCP and DCPD, agreed with literature spectra (carbonate peaks appeared in the IR of the HAP (Ca/P = 1.58) sample, which was analyzed to contain 0.9% CO<sub>3</sub><sup>2-</sup>).

Sample identity was also confirmed by chemical analyses for the Ca/P ratio using inductively coupled plasma (ICP) emission. The ICP method has an accuracy of 1–3% in the Ca/P ratio; molar Ca/P ratios obtained by this method for the nonstoichiometric HAP samples are given in parentheses, e.g., HAP (1.33).

The commercial MCPM sample had a Ca/P ratio of 0.42 (0.50 theoretical). The <sup>31</sup>P NMR revealed a substantial amount of phosphoric acid contaminant, which was removed by washing with anhydrous ethanol. X-ray powder diffraction confirmed the sample's identity after washing.

**NMR Spectra.** Spectra were obtained on a home-built double-resonance spectrometer employing a wide-bore 4.0-T (<sup>31</sup>P = 68.42 MHz) superconducting magnet. Magic-angle spinning spectra were acquired on ~0.3 cm<sup>3</sup> of tightly packed dry powders in a Beams-type rotor spun at speeds of 1–2.5 kHz, resulting in typical line widths of 1–3 ppm. Fluctuations in spinning speed and the vibrational stability of the spinning sample were monitored at times by a photoelectric tachometer. Proton-decoupling fields of ~1.0 mT were used, with typical decoupling times of 256 ms and spectral widths of 20 kHz. The time of contact between the <sup>1</sup>H and <sup>31</sup>P spin systems during proton enhancement (typically 0.1–10 ms) is referred to in the text as the cross-polarization time. Approximate T<sub>1</sub> values for spinning samples of HAP were measured by determining the signal null after a 180–τ–90 pulse sequence. The approximate matching condition for proton enhancement<sup>5</sup> was typically achieved by adjusting the <sup>31</sup>P transmitter power for maximum signal intensity. For the spectrum in Figure 4d,

the Hartmann–Hahn matching condition<sup>5</sup> was obtained by adjusting for equal 90° pulse lengths for <sup>1</sup>H and <sup>31</sup>P. The Hartmann–Hahn mismatch in Figure 4e was obtained by lowering the <sup>31</sup>P transmitter power from the level corresponding to matching. Chemical shifts were measured by replacing the rotor containing the sample with a rotor containing a small ampule of the reference, 85% H<sub>3</sub>PO<sub>4</sub>, and observing its resonance frequency in the absence of spinning.

For variable-temperature MAS-NMR work the nitrogen driving gas was precooled to ~-190 °C in a Dewar of liquid nitrogen and then heated downstream to the appropriate temperature with a heating coil interfaced to a temperature controller. Temperatures were measured to an estimated accuracy of ±3 °C with a copper-constantan thermocouple positioned about 2 cm from the rotating sample. The sample spinner, coil, and thermocouple, which were all mounted on the probe head, were thermally insulated from their surroundings by means of a glass Dewar fitted to the top of the probe and having a long gas exhaust port.

## Results

The <sup>31</sup>P NMR chemical shifts at room temperature for all samples are given in Table I, and typical spectra are shown in Figures 1–4. The results for individual compounds are given below.

**HAP.** Only one <sup>31</sup>P resonance with weak sidebands is observed for HAP (1.58) (Figure 1a) as well as for a commercial sample of HAP (Ca/P = 1.62), in agreement with the crystallographic equivalence of all the phosphate groups.<sup>9</sup> The isotropic chemical shift of HAP agrees with the value determined by using a colloidal suspension of HAP.<sup>10</sup>

A single <sup>31</sup>P resonance at the same shift, with weak sidebands, is also observed for the highly stoichiometric, carbonate-free HAP sample, which exists largely in the monoclinic form (Figure 1c). The three crystallographically inequivalent phosphorus atoms in this form<sup>11</sup> apparently have identical chemical shifts. This is reasonable, since the phosphate groups in the monoclinic form have the same neighbors as in the more common hexagonal form above. The main difference between

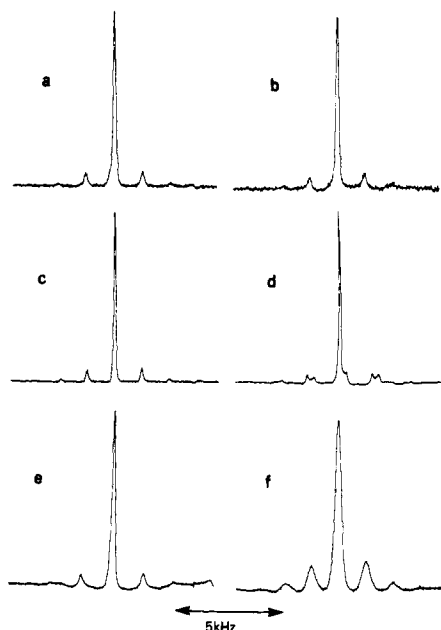


**Figure 1.**  $^{31}\text{P}$  MAS-NMR spectra of hydroxyapatite samples: (a) HAP(1.58) at 20 °C, spinning rate = 1.27 kHz, 90° pulse with decoupling, 1-min pulse interval, eight accumulations; (b) HAP(1.58) at -175 °C, proton enhanced, cross-polarization time = 0.5 ms, 10-s pulse repetition; (c) stoichiometric HAP (Ca/P = 1.66) at 20 °C, spinning rate = 1.23 kHz, 45° pulse with decoupling, 30-s pulse interval; (d) HAP(1.14) at 20 °C, proton enhanced, cross-polarization time = 5.0 ms, 2-s pulse repetition; (e) human dental enamel at 20 °C, 90° pulse with decoupling, 20-s pulse interval, 47 accumulations; (f) human dental enamel at -190 °C, proton enhanced, cross-polarization time = 1.0 ms, 20-s pulse repetition.

the two forms is in the long-range orientation of the  $\text{OH}^-$  groups.

The principal values of the shielding tensor were determined from  $^{31}\text{P}$  MAS-NMR spectra using a moments analysis of the sideband intensities<sup>4</sup> (Table I). The  $^{31}\text{P}$  chemical-shift anisotropy of all the HAP samples is small, as deduced from the weak intensities of the first pair of sidebands. An isolated, undistorted  $\text{PO}_4^{3-}$  group would, of course, have zero chemical-shift anisotropy.

The results on nonstoichiometric HAP samples and the variable-temperature study appear in a later section.

**FAP.** Only one  $^{31}\text{P}$  resonance is observed for FAP (Figure 2a), as expected (FAP is isostructural with HAP).<sup>12</sup> Synthetic FAP has a chemical shift identical with that of HAP, and a similarly small shift anisotropy as indicated by weak sideband intensities.

The mineral FAP sample exhibited marked differences compared with the synthetic FAP sample. The sideband intensities were considerably larger, and different for different portions of the mineral sample. Impurities in the mineral sample are presumably responsible for these differences.

**OCP.** The  $^{31}\text{P}$  MAS-NMR spectrum of OCP at room temperature shows two incompletely resolved peaks separated by 3.5 ppm (Figure 3a), in addition to sidebands. Increasing the cross-polarization time from 0.1 to 1.0 ms (keeping all other conditions constant) results in a less pronounced "dip" between the two peaks, indicating that a third peak between the two main peaks is growing in.

The sidebands observed are somewhat broader than the central peaks, and do not show any splitting into two partially resolved peaks. Although the sidebands appeared to belong predominantly to the high-field peak, "difference spectroscopy" was used to definitively obtain the sidebands associated with a given peak. This method relies upon the ability to preferentially enhance various peaks by changing the cross-polarization time. Figures 3a and 3b show how the low-field

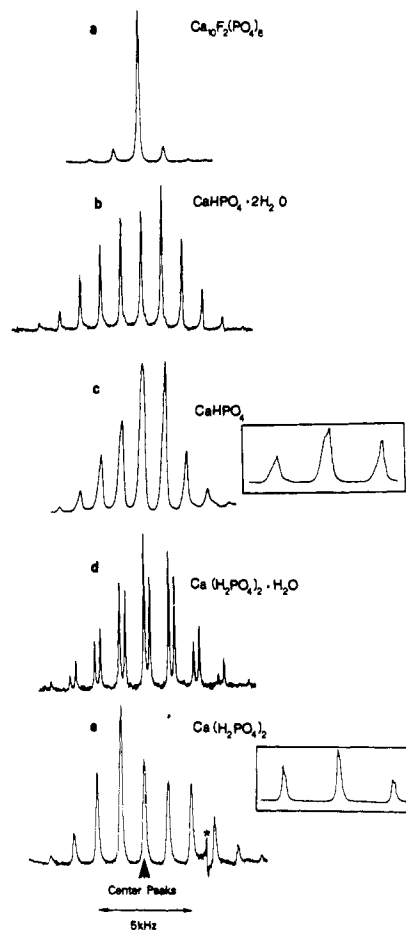


**Figure 2.**  $^{31}\text{P}$  MAS-NMR spectra of calcium phosphates at 20 °C: (a) synthetic FAP, 90° pulse, 10-s pulse interval; (b) DCPD, 90° pulse with decoupling, spinning rate = 1.10 kHz, 6-s pulse interval; (c) DCPA, spinning rate = 1.14 kHz, proton enhanced, cross-polarization time = 0.5 ms, 5-s pulse repetition; inset is expansion of proton-enhanced spectrum obtained with spinning rate = 1.37 kHz, cross-polarization time = 2.5 ms, 4-s pulse repetition, showing two partially resolved peaks, relative intensities of two peaks change with cross-polarization time; (d) MCPM, spinning rate = 1.33 kHz, proton enhanced, cross-polarization time = 0.5 ms, 1-min pulse repetition; (e) MCPA, proton enhanced, cross-polarization time = 5.0 ms, 10-s pulse repetition (asterisk indicates artifact). Inset is expansion of proton-enhanced spectrum obtained with spinning rate = 2.12 kHz, cross-polarization time = 1.0 ms, 5-s pulse repetition, showing two partially resolved peaks.

peak is preferentially enhanced upon increasing the cross-polarization time from 0.5 to 5.0 ms. Upon subtracting digitally spectrum 3b from spectrum 3a, the "difference spectrum" that results (Figure 3c) shows only the high-field peak and its associated sidebands. The spectra are scaled appropriately to eliminate the low-field peak and avoid negative intensities.

Determining the relative number of phosphates contributing to each peak is complicated by the differential proton enhancement. In order to obtain peak intensities proportional to the number of phosphates, a simple 90° pulse with decoupling was used. The interval between successive pulses was 5 min, which seemed to be sufficiently long to exclude  $T_1$  effects by comparison with a spectrum obtained at 1-min intervals. The integrated intensities of the low-field and high-field peaks were measured assuming various possible peak shapes. The results indicate that the high-field peak arises from roughly  $1/3$  of the total phosphates.

The  $^{31}\text{P}$  MAS-NMR spectra obtained near liquid nitrogen temperatures are also strongly dependent upon the cross-polarization time used. At -179 °C with a cross-polarization time of 0.1 ms, only one main peak with low sideband intensity is seen. Its position is very slightly upfield of the low-field peak

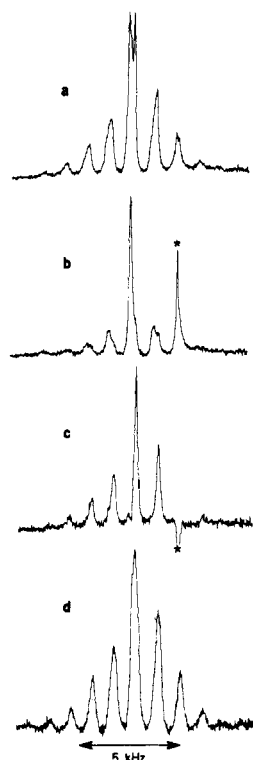


**Figure 3.** Proton-enhanced  $^{31}\text{P}$  MAS-NMR spectra of OCP: (a) 20 °C, cross-polarization time = 1.0 ms, 5-s pulse repetition; (b) 20 °C, cross-polarization time = 5.0 ms, 5-s pulse repetition (asterisk indicates zero-frequency artifact); (c) "difference spectrum" at 20 °C, obtained by subtracting scaled spectrum in (b) from spectrum in (a) (asterisk indicates zero-frequency artifact); (d) -165 °C, cross-polarization time = 1.0 ms, 5-s pulse repetition, main component is high-field peak.

of OCP, and it presumably corresponds to the "third peak" at room temperature mentioned above.

Increasing the cross-polarization time to 1.0 ms at -176 °C results in the appearance of the high-field peak, with considerable sideband intensity. A further increase in the cross-polarization time to 5.0 ms appears to increase the contribution from the low-field peak. Since the peak observed with these cross-polarization times is fairly broad (half-height line width = 7 ppm), at least partly due to overlapping resonances, the high-field and low-field peaks are not distinctly resolved in these spectra. This is also true for a spectrum obtained at -175 °C using a simple 90° pulse with decoupling (pulse repetition = 2.5 min).

The intensity of the sidebands increases at lower temperatures. For a spectrum obtained at -165 °C with a cross-polarization time of 1.0 ms (Figure 3d), the sidebands are significantly more intense than those observed in the "difference spectrum" at room temperature (Figure 3c); the spinning speed is nearly identical for both spectra. However, it is not possible to use the low-temperature sideband intensities to calculate an accurate shift anisotropy for the high-field peak, since the low-temperature spectra are not resolved sufficiently to obtain a "difference spectrum"; the low-field peak may be contributing somewhat to the observed spectrum.

**DCPD.** There has been some controversy over the crystal structure of DCPD, but the most recent neutron diffraction study established a noncentrosymmetric space group with only one crystallographically inequivalent phosphate.<sup>13</sup> Kohler<sup>14</sup> measured the  $^{31}\text{P}$  chemical shift tensors on a single crystal, observing two resonances with calculated isotropic chemical shifts (ideally equivalent) of 8.3 and 9.3 ppm. We measured an isotropic shift of 1.7 ppm, and attribute the difference between these values to the relatively large errors in the single-crystal study arising from the broad lines. The principal values

of the shielding tensor determined from the  $^{31}\text{P}$  MAS-NMR spectrum (Figure 2b) using a moments analysis of the sideband intensities<sup>4</sup> are in reasonable agreement with those determined from the single-crystal study (Table I).

**DCPA.** A neutron diffraction study of this compound established two crystallographically distinct phosphate groups.<sup>15</sup> Half of the phosphates are bonded to one hydrogen as  $\text{HPO}_4^{2-}$  groups, while the other half have one proton in a symmetrically bridging hydrogen bond and one proton statistically distributed between two centrosymmetric positions. Static disorder involving the latter proton is likely, and would result in further inequivalences among the phosphate groups. A slight increase in the  $^1\text{H}$  NMR line width upon cooling to -170 °C suggests the presence of proton motions.<sup>16</sup>

The  $^{31}\text{P}$  MAS-NMR spectrum shows two partially resolved peaks with intense sidebands, corresponding to at least two types of phosphates (Figure 2c). Since only half of the phosphates are isolated  $\text{HPO}_4^{2-}$  groups, and the two NMR peaks are not resolved, calculation of the chemical-shift anisotropy using the sideband intensities is not justified. However, it is qualitatively apparent from the sideband intensities that the shift anisotropies in DCPA are considerably larger than that of HAP (Figure 1a).

**MCPM.** The proton-enhanced  $^{31}\text{P}$  MAS-NMR spectrum obtained using a long delay (1 min) between pulse cycles shows two peaks of approximately equal intensities at -0.1 and -4.6 ppm with similar, sizable sideband intensities (Figure 2d). The principal values of the shielding tensors calculated using the moments analysis are given in Table I. The two peaks correspond to the two crystallographically inequivalent  $\text{H}_2\text{PO}_4^-$  groups seen in the neutron diffraction crystal structure.<sup>17</sup> There are differences in the hydrogen bonding of the two groups: one  $\text{H}_2\text{PO}_4^-$  accepts two hydrogen-bonding protons from a water molecule and the other  $\text{H}_2\text{PO}_4^-$ , whereas the second  $\text{H}_2\text{PO}_4^-$  donates one hydrogen-bonding proton. The significant chemical-shift difference between the phosphates is most likely due to these differences in hydrogen bonding.

**MCPA.** The  $^{31}\text{P}$  MAS-NMR spectrum shows two partially resolved resonances separated by about 1.0 ppm (Figure 2e). This observation agrees with the two crystallographically inequivalent phosphates seen in the X-ray and neutron diffraction structures.<sup>18</sup> One type consists of dimeric  $\text{H}_2\text{PO}_4^-$  groups; the other type is a hydrogen-bonded chain of phosphates, with symmetrically bridging protons. The two peaks overlap too much to calculate reliable individual chemical-shift anisotropies, but they are clearly large compared to that of HAP.

**Nonstoichiometric HAP.** The most striking feature of the  $^{31}\text{P}$  MAS-NMR spectra at room temperature of the nonstoichiometric samples HAP(1.46) and HAP(1.33) (Figure 4b) is their similarity to the spectra of stoichiometric HAP discussed above. The chemical shifts are identical, and the sideband intensities are small compared to those of DCPD, DCPA, MCPM, and MCPA. This is true for spectra obtained by proton enhancement with cross-polarization times ranging from 0.5 to 5.0 ms as well as by simple 90° pulses with decoupling and long (1 min) pulse intervals.

For the lowest ratio nonstoichiometric sample, HAP(1.14), the main peak plus sidebands resemble those of the other HAP samples. However, there is present in addition a small upfield peak with relatively intense sidebands (Figure 1d). A spectrum exhibiting mainly the weak upfield peak could be obtained by cross-polarizing both peaks, inverting the magnetization of both resonances with a 90° pulse, allowing the magnetization of the main resonance to decay to zero by a  $T_1$  process, and applying a second 90° pulse for observation. The upfield peak has a chemical shift and sideband intensity comparable to those of DCPA; the X-ray powder diffraction pattern of this sample did show one very weak reflection attributable to DCPA, in addition to the HAP reflections. Therefore,  $^{31}\text{P}$  MAS-NMR

can be a more sensitive technique than X-ray for detecting small amounts of components. The DCPA is crudely estimated to be less than 15% of the sample, which means that by itself it could only account for a nonstoichiometric Ca/P ratio greater than 1.57. Clearly the main resonance arises from a highly nonstoichiometric HAP.

A large number of  $^{31}\text{P}$  MAS-NMR spectra of HAP samples were obtained near liquid nitrogen temperature under a variety of conditions. No differences in isotropic shifts were observed (or expected), but significant increases in sideband intensities were observed for highly nonstoichiometric samples under certain conditions.

When a simple  $90^\circ$  (or  $45^\circ$ ) pulse with decoupling and a 1-min pulse interval is used, no significant increase in sideband intensity is observed for HAP(1.46) at  $-177^\circ\text{C}$  or for HAP(1.33) at  $-187^\circ\text{C}$  relative to HAP(1.58) at room temperature and comparable spinning speeds. A comparison of Figures 1a, 1c, 4b, and 4c illustrates this behavior, which is also seen for HAP(1.14).

In contrast to these observations, the proton-enhanced spectra of HAP(1.33) show marked increases in sideband intensities. This effect is shown in Figure 4d, obtained at  $-187^\circ\text{C}$  with a cross-polarization time of 0.5 ms. This spectrum was obtained under conditions where the Hartmann-Hahn condition for cross-polarization is met ("matched"). The effect of intentionally mismatching the Hartmann-Hahn condition<sup>19</sup> is to increase the sideband intensities further (Figure 4e). A similar, although considerably smaller, increase in sideband intensities is observed under mismatch conditions for this sample at room temperature.

The proton-enhanced spectrum of HAP(1.46) at  $-185^\circ\text{C}$  also shows an increase in sideband intensities, especially under Hartmann-Hahn mismatch conditions. This increase is less marked than that observed for HAP(1.33). The proton-enhanced spectrum of HAP(1.14) at  $-176^\circ\text{C}$  has dramatically larger sideband intensities than those observed at room temperature, but overlap of peaks from the  $\text{CaHPO}_4$  component makes it difficult to quantitate the increase in intensity of sidebands associated with the main peak.

These observations indicate a heterogeneity of phosphate groups. If all phosphate groups were equivalent, with identical shift anisotropies, then the sideband intensities relative to the central peak should remain constant at constant spinning frequency regardless of the conditions employed to obtain the spectrum. Since this is not observed, there must be at least two types of phosphate groups whose isotropic shifts overlap but which have significantly different shift anisotropies.

In contrast to the increase in sideband intensities observed using proton enhancement at low temperatures for HAP(1.33), the HAP(1.58) sample shows no such increase under similar conditions (Figure 1b). This implies that there is no heterogeneity of phosphate groups as observed in the highly nonstoichiometric HAP samples.

**$T_1$  Measurements.** The  $T_1$  values for  $^{31}\text{P}$  in HAP varied considerably, from about 1.5 min in human enamel to anywhere from 1 to 22 s in synthetic HAP samples (including nonstoichiometric samples). Paramagnetic impurities are not present in the synthetic samples in significant amounts (unless  $\text{O}^-$  is present), so that differences in composition and motions are presumably responsible for the wide variation in  $T_1$  values. When the  $T_1$  of  $^{31}\text{P}$  in solid calcium phosphates is long, proton enhancement offers a significant sensitivity advantage over simple  $90^\circ$  pulses, since the pulse repetition rate is limited by the generally shorter  $T_1$  values for  $^1\text{H}$ .

**Human Enamel.** The  $^{31}\text{P}$  MAS-NMR spectrum of human enamel at room temperature (Figure 1e) shows a single peak with weak sidebands about 0.5 ppm downfield from that of HAP and with a half-height width of 3 ppm. The sideband intensities are comparable to those of HAP. Figure 1f shows

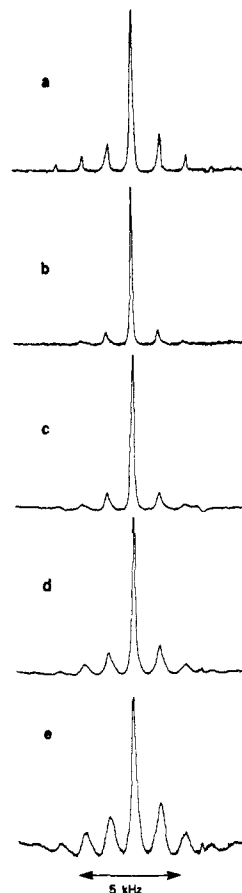


**Figure 4.**  $^{31}\text{P}$  MAS-NMR spectra of DCPD/HAP mixture and nonstoichiometric hydroxyapatite: (a) mixture of 3DCPD/1HAP ( $\text{HPO}_4^{2-}/\text{PO}_4^{3-} = 1/2$ ) at  $20^\circ\text{C}$ , spinning rate = 1.28 kHz,  $45^\circ$  pulse with decoupling, 1-min pulse interval; (b) HAP(1.33) at  $20^\circ\text{C}$ , spinning rate = 1.27 kHz,  $45^\circ$  pulse with decoupling, 1-min pulse interval; (c) HAP(1.33) at  $-187^\circ\text{C}$ , spinning rate = 1.28 kHz,  $45^\circ$  pulse with decoupling, 1-min pulse interval, 4 accumulations; (d) HAP(1.33) at  $-187^\circ\text{C}$ , proton enhanced, spinning rate = 1.27 kHz, cross-polarization time = 0.5 ms, Hartmann-Hahn matched (see text), 15-s pulse repetition; (e) HAP(1.33) at  $-187^\circ\text{C}$ , proton enhanced, spinning rate = 1.27 kHz, cross-polarization time = 0.5 ms, Hartmann-Hahn mismatched (see text), 10-s pulse repetition.

the increase in sideband intensities observed in a proton-enhanced spectrum at  $-190^\circ\text{C}$ ; this increase is more marked under conditions of Hartmann-Hahn mismatch. These changes in relative sideband intensities indicate that the enamel sample contains different types of phosphate groups with different shift anisotropies but with overlapping isotropic shifts. This heterogeneity may be responsible for the slight downfield shift of the center of the enamel resonance relative to HAP. The groups with the larger shift anisotropy could be  $\text{HPO}_4^{2-}$  groups (see discussion of nonstoichiometric HAP), but a conclusive (and quantitative) identification is not yet possible.

## Discussion

The  $^{31}\text{P}$  isotropic chemical shifts of calcium phosphates tend to move upfield upon protonation of the phosphate group, although exceptions occur. This is consistent with the observed upfield shifts upon successive protonation of the phosphate group *in solution*, the chemical-shift difference between  $\text{PO}_4^{3-}$  and  $\text{H}_3\text{PO}_4$  being 6 ppm.<sup>20</sup> Furthermore, the chemical-shift anisotropy is small for  $\text{PO}_4^{3-}$  groups and much larger for both  $\text{HPO}_4^{2-}$  and  $\text{H}_2\text{PO}_4^-$  groups. This generalization is further supported by our preliminary observations of  $^{31}\text{P}$  MAS-NMR spectra of  $\beta\text{-Ca}_3(\text{PO}_4)_2$  and  $\text{Ca}_4(\text{PO}_4)_2\text{O}$ , whose shift anisotropies are smaller than those of protonated phosphate groups.

It is interesting to note that the variation in shift anisotropies for calcium phosphates is about an order of magnitude greater than the variation in isotropic shifts.

**OCP.** The assignment of the  $^{31}\text{P}$  resonances for OCP draws upon the reported single-crystal X-ray diffraction study.<sup>21</sup> In the asymmetric unit,  $\text{Ca}_8\text{H}_2(\text{PO}_4)_6 \cdot 5\text{H}_2\text{O}$ , four of the phosphates belong to an "apatitic layer" that closely resembles part of the structure of HAP, whereas the other two phosphates adjoin a region called the "water layer", containing waters of hydration. The two acidic hydrogen atoms have not been located in the structure.

We assign the high-field  $^{31}\text{P}$  NMR peak to the two acidic phosphate groups on the basis of (1) an observed intensity ratio of about 1/3, in agreement with two  $\text{HPO}_4^{2-}$  groups and four  $\text{PO}_4^{3-}$  groups; (2) the tendency of protonation to produce upfield shifts; (3) the short cross-polarization time observed for proton enhancement, indicative of nearby protons; (4) the larger sideband intensities observed for the high-field peak relative to the low-field peak, indicating a shift anisotropy greater than that expected for a  $\text{PO}_4^{3-}$  group.

The low-field peak, which has a chemical shift close to that of HAP, is assigned to the "apatitic layer"  $\text{PO}_4^{3-}$  groups. The "third peak" mentioned above, which occurs very slightly upfield of the low-field peak, may correspond to "apatitic layer"  $\text{PO}_4^{3-}$  groups that are near protons of water molecules or adjacent  $\text{HPO}_4^{2-}$  groups. This assignment is supported by the low-temperature spectrum of the "third peak," which shows low sideband intensities characteristic of  $\text{PO}_4^{3-}$  groups but a short cross-polarization time indicative of nearby protons.

Although the high-field peak has more intense sidebands than the low-field peak, the sidebands are significantly less intense than those observed for DCPD (and DCPA) at similar spinning speeds. This is surprising, since an isolated  $\text{HPO}_4^{2-}$  group might be expected to have a shift anisotropy similar to that of DCPD, regardless of the details of the crystal structure. One possible explanation is that  $\text{HPO}_4^{2-}$  groups in OCP are undergoing atomic or molecular motions which reduce the full shift anisotropy by an averaging process. These motions could be a jump of the proton to another site on the same or an adjacent phosphate group, or a rotation of an  $\text{HPO}_4^{2-}$  group. Such motions have been observed in NMR studies of the ferroelectric  $\text{KD}_2\text{PO}_4$  in the paraelectric phase.<sup>22</sup> The protons of water molecules in OCP might also be involved.

The low-temperature  $^{31}\text{P}$  MAS-NMR spectra were obtained in the hopes of "freezing out" any motion that reduced the apparent shift anisotropy at room temperature. The increase in sideband intensities observed at  $-165^\circ\text{C}$  (Figure 3d) relative to the room-temperature spectrum (Figure 3c) suggests that some motion is at least partially frozen out at low temperature. The sideband intensities at  $-165^\circ\text{C}$  approach those seen for DCPA, and could actually be larger if the low-field peak contributes significantly to the spectrum.

One possible complication in this interpretation arises from the assignment of the high-field peak to *two*  $\text{HPO}_4^{2-}$  groups. If these had widely different shift anisotropies (perhaps because of motions), then the increase in sideband intensities at low temperatures might be due to a preferential enhancement of the group with the larger anisotropy.

An interesting possibility arises from the ability of OCP to lose part of its waters of hydration at higher temperatures, resulting in partially collapsed structures.<sup>21,23,24</sup> The existence of molecular or atomic motions in OCP might be confirmed by  $^{31}\text{P}$  MAS-NMR if partially dehydrated OCP exhibits more hindered, slower motions.

**Nonstoichiometric HAP.** The numerous experimental studies of the nature of nonstoichiometric HAP have been reviewed.<sup>3</sup> Four proposals for the constitution of nonstoichiometric HAP are (1)  $\text{Ca}^{2+}$  vacancies in a HAP lattice, with

charge balance maintained by loss of  $\text{OH}^-$  and/or addition of a proton; (2) stoichiometric HAP with surface-adsorbed acid phosphate groups; (3) epitaxial intergrowths of OCP and stoichiometric HAP; (4) mixtures of stoichiometric HAP with more acidic phases such as DCPD and DCPA. Although the small particle size of nonstoichiometric HAP creates experimental ambiguities, and although the exact mechanism of nonstoichiometry may depend upon the method of sample preparation,<sup>2</sup> many studies support the validity of proposal (1).

In particular, for nonstoichiometric HAP with  $\text{Ca}/\text{P} = 1.40$ – $1.50$ , Berry<sup>25</sup> concluded on the basis of IR and thermal analysis that the following general compositional formula applied:  $\text{Ca}_{9-x}(\text{HPO}_4)_{1+2x}(\text{PO}_4)_{5-2x}(\text{OH})$ . No other phases, including OCP, were observed in these samples.

The  $^{31}\text{P}$  MAS-NMR spectra of HAP(1.46) and HAP(1.33) show only a single peak with weak sidebands at the chemical shift of stoichiometric HAP. Since the  $^{31}\text{P}$  MAS-NMR spectra of OCP, DCPA, MCPM, and MCPA obtained under the same conditions show peaks with chemical shifts resolvable from that of HAP, we conclude that these phases are not present in HAP(1.46) and HAP(1.33). The  $^{31}\text{P}$  resonance of DCPD would not be resolved from that of HAP; however, the large sideband intensities of DCPD rule out its presence in these nonstoichiometric HAP samples. If HAP(1.33) were a mixture of stoichiometric HAP and DCPD, the two compounds would exist in the ratio 6DCPD/1HAP. Figure 4a shows that even for a mixture with the lower ratio 3DCPD/1HAP the sideband intensities are much larger than those observed for HAP(1.33).

The absence of more acidic compounds in HAP(1.46) and HAP(1.33) agrees with our IR and X-ray data. The tentative identification of DCPA in HAP(1.14) is consistent with Berry's observation<sup>25</sup> that nonstoichiometric HAP samples with  $\text{Ca}/\text{P}$  less than 1.40 tend to have more acidic phases present. It should be noted that the method of preparation of the nonstoichiometric samples could have resulted in a dehydration of any OCP present;<sup>23,24</sup> we intend to investigate this possibility.

Since our results rule out proposals (3) and (4) above, we consider proposal (1) next. If the general compositional formula given above applies to HAP(1.33), equal numbers of  $\text{HPO}_4^{2-}$  and  $\text{PO}_4^{3-}$  groups would be present. If, instead, we assume that both  $\text{OH}^-$  groups of HAP might be lost (perhaps by formation of  $\text{H}_2\text{O}$ ) to yield a general compositional formula  $\text{Ca}_{9-x}(\text{HPO}_4)_{2x}(\text{PO}_4)_{6-2x}$ , we obtain for HAP(1.33) a  $\text{HPO}_4^{2-}/\text{PO}_4^{3-}$  ratio of 1/2. This value represents the *lowest* ratio consistent with proposal (1), unless the added proton does not form discrete  $\text{HPO}_4^{2-}$  groups (see below).

The spectrum of a DCPD/HAP mixture in Figure 4a shows what the spectrum of HAP(1.33) should resemble if the  $\text{HPO}_4^{2-}$  groups in nonstoichiometric HAP had the same shift anisotropy as in DCPD, had isotropic shifts overlapping that of HAP, and were present in the ratio 1 $\text{HPO}_4^{2-}$ /2 $\text{PO}_4^{3-}$ . The observed sideband intensities of HAP(1.33) are clearly smaller (Figure 4b). It is not likely that rigid  $\text{HPO}_4^{2-}$  groups in nonstoichiometric HAP would have a shift anisotropy greatly reduced from that of DCPD, since our results on other compounds support the notion that the magnitude of the shift anisotropy of phosphate groups depends primarily upon the protonation state rather than upon crystal-lattice effects.

Thus, the observed sideband intensities seem to be significantly less than those anticipated from both compositional formulas given above for proposal (1), especially the first one. Proposal (2) would not yield better agreement, since the relative amounts of  $\text{HPO}_4^{2-}$  would be even larger than those calculated from the compositional formulas (it also would have difficulties in accounting for the low  $\text{Ca}/\text{P}$  ratios of these samples, whose specific surface area is typically<sup>6</sup> less than 100

$\text{m}^2/\text{g}$ ). However, there are two possibilities that would render the NMR results consistent with proposal (1).

(1) Instead of discrete  $\text{HPO}_4^{2-}$  groups, other forms such as phosphate groups with symmetrically bridging protons could be present in nonstoichiometric HAP. This would be consistent with our results, if the shift anisotropy of these phosphates were then much smaller than that of DCPD, a possibility we cannot rule out. The formation of  $\text{H}_3\text{O}^+$  groups at  $\text{OH}^-$  lattice sites is unlikely, since the hydronium ion is usually found only in very acid solids.<sup>26</sup>

(2) Discrete  $\text{HPO}_4^{2-}$  groups could be present in nonstoichiometric HAP if atomic or molecular motions reduce the  $\text{HPO}_4^{2-}$  shift anisotropy by an averaging process (cf. discussion of OCP).

The results at low temperature indicate at least two types of phosphate groups for the nonstoichiometric HAP samples. We believe that the component with more intense sidebands, and hence larger shift anisotropy, is probably  $\text{HPO}_4^{2-}$ , since (1) it has more intense sidebands than observed for  $\text{PO}_4^{3-}$  in a variety of compounds; (2) its intensity increases as the degree of nonstoichiometry increases; (3)  $\text{H}_2\text{PO}_4^-$  would be less likely to overlap with the  $\text{PO}_4^{3-}$  resonance. The sideband intensities in Figure 4e provide a lower limit for the shift anisotropy of the  $\text{HPO}_4^{2-}$  groups. The fact that the sideband intensities are largest in the proton-enhanced spectra at low temperature is evidence for the presence of motion at room temperature, unless for some reason preferential enhancement of the  $\text{HPO}_4^{2-}$  component is greater at low temperature.

The  $90^\circ$  pulse experiments at low temperature show that the amount of the component ascribed to  $\text{HPO}_4^{2-}$  is small relative to the  $\text{PO}_4^{3-}$  component, smaller than the compositional formulas above would predict (unless the  $T_1$  of the  $\text{HPO}_4^{2-}$  groups is very long). A plausible explanation of these results is that the motions are not being completely frozen out at temperatures near that of liquid nitrogen. In the proton-enhanced experiments we may be witnessing a small fraction of the  $\text{HPO}_4^{2-}$  groups whose motions are frozen out. It is worth pointing out that, since the pH necessarily varied during the synthesis of these nonstoichiometric HAP samples, they need not be homogeneous.

We conclude that proposal (1) can best account for the NMR results, if we assume that the protons added do not form rigid, discrete  $\text{HPO}_4^{2-}$  groups. Determining the location of these protons in the nonstoichiometric HAP lattice is the object of experiments we are planning. Washing the samples thoroughly should minimize any contribution from surface-adsorbed phosphates. Because of the experimental difficulties associated with going below liquid nitrogen temperature in the MAS-NMR experiment, we are preparing deuterated nonstoichiometric HAP samples, since any motions may be more readily frozen out.<sup>22</sup> Also,  $^1\text{H}$  and  $^2\text{H}$  MAS-NMR may be capable of providing further evidence for proton motions in this class of compounds.

**Implications for the Analysis of Mineralized Tissue.**  $^{31}\text{P}$  MAS-NMR is a promising technique for the analysis of calcium phosphates in mineralized tissue, as it should be possible to quantitate the relative amounts of various components in untreated samples of powders. Since the  $^{31}\text{P}$  chemical shift is primarily a local parameter, small particle sizes will not present the problems encountered by X-ray diffraction methods.

The likely limitations of the NMR method are a fairly large sample requirement,  $\sim 0.1$  g, and the small isotropic chemical shift range of the calcium phosphates. The latter problem may be more severe in biological samples because of broader peaks. Herzfeld et al.<sup>1</sup> have shown that in this case the sideband in-

intensities can be used to quantitate components with overlapping isotropic shifts but different shift anisotropies. Another approach would be to heat samples to form DCPA from DCPD, making it easier to quantitate mixtures of HAP and DCPD (cf. Figures 1d and 4a). At higher temperatures  $\text{HPO}_4^{2-}$  groups condense to form pyrophosphate; we have detected and quantitated upfield pyrophosphate resonances from samples of heated calcium phosphates.

The wide variation in  $^{31}\text{P}$   $T_1$ 's observed for various samples of HAP makes it likely that other relaxation parameters also vary. Thus, proton enhancement may not be suitable for quantitating mixtures of calcium phosphates if these parameters are sufficiently different between the standard and the unknown. In addition, any mismatch in the Hartmann-Hahn condition would affect quantitation. We believe that simple  $90^\circ$  pulses with decoupling represent a more satisfactory method of quantitation.

An increase in the NMR resolution would clearly be advantageous. Preliminary results show that the resonances of several amorphous calcium phosphates are broader than those of the crystalline samples investigated here. If this is due to a distribution of phosphate chemical shifts, then the resolution limitation in this case is intrinsic. Even under this circumstance, the sideband intensities and proton-enhancement characteristics may provide additional information about the degree of protonation and composition of these compounds.

**Acknowledgments.** We wish to thank Dr. E. C. Moreno and B. O. Fowler for providing several samples, and Dr. Gerhard Wagner and George Rudolph for help in constructing the variable-temperature apparatus. J.S.W. and W.P.R. acknowledge NIH Grant GM-16552 for partial support of this research.

## References and Notes

- Herzfeld, J.; Roufosse, A.; Haberkorn, R. A.; Griffin, R. G.; Glimcher, M. J. *Proc. R. Soc. London, Ser. B*, in press.
- Brown, W. E.; Chow, L. C. *Annu. Rev. Mater. Sci.* **1976**, *6*, 213-236.
- Kibby, C. L.; Hall, W. K. In "The Chemistry of Biosurfaces", Hair, M. L., Ed.; Marcel Dekker: New York, 1972; Vol. 2, pp 663-729.
- Maricq, M. M.; Waugh, J. S. *J. Chem. Phys.* **1979**, *70*, 3300-3316.
- Pines, A.; Gibby, M. G.; Waugh, J. S. *J. Chem. Phys.* **1973**, *59*, 569-590.
- Bett, J. A. S.; Christner, L. G.; Hall, W. K. *J. Am. Chem. Soc.* **1967**, *89*, 5535-5541.
- Fowler, B. O. *Inorg. Chem.* **1974**, *13*, 207-214.
- Moreno, E. C.; Kresak, M.; Zaradnik, R. T. *Caries Res., Suppl.* **1977**, *142-171*.
- Kay, M. I.; Young, R. A.; Posner, A. S. *Nature (London)* **1964**, *204*, 1050-1052.
- Yesinowski, J. P., to be published.
- Elliott, J. C.; Mackie, P. E.; Young, R. A. *Science* **1973**, *180*, 1055-1057.
- Sudarsanan, K.; Mackie, P. E.; Young, R. A. *Mater. Res. Bull.* **1972**, *7*, 1331-1338.
- Curry, N. A.; Jones, D. W. *J. Chem. Soc. A* **1971**, 3725-3729.
- Kohler, S. J. Ph.D. Thesis, University of California, Berkeley, 1975.
- Catti, M.; Ferraris, G.; Filhol, A. *Acta Crystallogr., Sect. B* **1977**, *33*, 1223-1229.
- Blinc, R.; Hadži, D. *Spectrochim. Acta*, **1960**, *16*, 853-862.
- Schroeder, L. W.; Prince, E.; Dickens, B. *Acta Crystallogr., Sect. B* **1975**, *31*, 9-12.
- Dickens, B.; Prince, E.; Schroeder, L. W.; Brown, W. E. *Acta Crystallogr., Sect. B* **1973**, *29*, 2057-2070.
- Demco, D. E.; Tegenfeldt, J.; Waugh, J. S. *Phys. Rev. B* **1975**, *11*, 4133-4151.
- Crutchfield, M. M.; Callis, C. F.; Irani, R. R.; Roth, G. C. *Inorg. Chem.* **1962**, *1*, 813-817.
- Brown, W. E. *Nature (London)* **1962**, *196*, 1048-1050.
- Blinc, R.; Pirš, J. *J. Chem. Phys.* **1971**, *54*, 1535-1539.
- Brown, W. E.; Smith, J. P.; Lehr, J. R.; Frazier, A. W. *Nature (London)* **1962**, *196*, 1050-1055.
- Fowler, B. O.; Moreno, E. C.; Brown, W. E. *Arch. Oral Biol.* **1966**, *11*, 477-492.
- Berry, E. E. *J. Inorg. Nucl. Chem.* **1967**, *29*, 1585-1590.
- Elliott, J. C. *Calcif. Tissue Res.* **1969**, *3*, 293-307.